



# HHS Public Access

Author manuscript

*Ophthalmol Retina*. Author manuscript; available in PMC 2021 November 01.

Published in final edited form as:

*Ophthalmol Retina*. 2020 November ; 4(11): 1069–1082. doi:10.1016/j.oret.2020.04.029.

## Correlation of Quantitative Measurements with Diabetic Disease Severity Utilizing Multiple En-Face OCTA Image Averaging

Jesse J. Jung, MD<sup>1,2</sup>, Daryle Jason G. Yu, MD<sup>3</sup>, Anne Zeng, BS<sup>1</sup>, Michael H. Chen, OD<sup>4</sup>, Yue Shi, MD, PhD<sup>5</sup>, Marco Nassisi, MD<sup>5,6</sup>, Kenneth M. Marion, MS, MBA<sup>5</sup>, Srinivas R. Sadda, MD<sup>5,7</sup>, Quan V. Hoang, MD, PhD<sup>3,8</sup>

<sup>1</sup>East Bay Retina Consultants Inc., Oakland, CA

<sup>2</sup>Department of Ophthalmology, University of California, San Francisco, San Francisco, CA

<sup>3</sup>Singapore Eye Research Institute, Singapore National Eye Centre, Duke-NUS Medical School, Singapore

<sup>4</sup>Silicon Valley Eyecare, Santa Clara, CA

<sup>5</sup>Doheny Eye Institute, Los Angeles, CA

<sup>6</sup>Department of Clinical Sciences and Community Health, University of Milan, Milan, Italy

<sup>7</sup>Department of Ophthalmology, David Geffen School of Medicine at UCLA, Los Angeles, CA

<sup>8</sup>Department of Ophthalmology, Edward S. Harkness Eye Institute, Columbia University College of Physicians and Surgeons, New York, NY

### Abstract

**Purpose:** To evaluate the effect of averaging en-face optical coherence tomography angiography (OCTA) images on quantitative measurements of the retinal microvasculature and their correlation to diabetic retinopathy (DR) disease severity.

**Design:** Cross-sectional cohort study

**Participants:** 105 eyes (65 patients) with 28 eyes from 19 healthy, aged-matched controls, 14 eyes from 9 diabetics without DR and 63 eyes from 37 diabetics with varying levels of DR.

**Methods:** Spectral-domain OCTA images with uniform illumination, good foveal centration, and no macular edema or significant motion artifact were acquired 5 times with the 3×3 mm scan pattern on the CIRRUS™ 5000 HD-OCT with AngioPlex (Carl Zeiss Meditec, Dublin, CA) software. En-face images of the superficial retinal layer (SRL) and deep retinal layer (DRL) were

---

Correspondence/reprints should be addressed to: Jesse J. Jung, M.D., East Bay Retina Consultants, Inc., 3300 Telegraph Ave., Oakland, CA 94609, Phone: 510-444-1600, Fax: 510-444-5117, jung.jesse@gmail.com.

This work was presented at the annual American Academy of Ophthalmology Meeting, 2019, October 12–15, San Francisco, CA.

Conflict of Interest:

JJJ: Consultant: Carl Zeiss Meditec, Inc., Alimera Sciences, Allergan, Google; DJGY: Employment: Support from Johnson and Johnson Vision Care; AZ: None; MHC: Employment: Topcon Medical Systems, Inc.; YS: No financial disclosures; MN: No financial disclosures; KM: No financial disclosures; SRS: Consultant: Optos, Heidelberg, Centervue, Allergan, Amgen, Roche/Genentech, Novartis, Regeneron, 4DMT and Research Support: Carl Zeiss Meditec, Inc.; QVH: Research Support: Johnson and Johnson Vision Care

registered and averaged. Included eyes had a signal strength  $\geq 7$ . Vessel length density (VLD), perfusion density (PD) and foveal avascular zone (FAZ) parameters were measured on averaged versus single OCTA images. Pearson correlation coefficient compared the two groups. Univariate and multivariate linear regression correlated quantitative metrics to DR severity and best corrected visual acuity (BCVA).

**Results:** 84 eyes (55 patients) met the inclusion criteria. Almost uniformly, lower VLD and PD parameters were significantly associated with worse DR severity and BCVA. Multivariable linear regression for DR severity resulted in an  $R^2$  value of 0.82 and 0.77 for single and averaged groups, respectively. No variables remained significantly associated with DR severity in multivariate analysis with single images but in averaged images, increased superior SRL PD significantly predicted worse DR severity (coefficient 52.7,  $p=0.026$ ). Multivariate linear regression for BCVA had an  $R^2$  value of 0.42 and 0.47 for single and averaged groups, respectively. FAZ size was not associated with DR severity when single OCTA images ( $p=0.98$ ) were considered, but was highly associated when using averaged images (coefficient 6.18,  $p<0.001$ ). FAZ size was predictive for logMAR BCVA with averaged images (0.21,  $p=0.004$ ), but not with single images ( $p=0.31$ ).

**Conclusions:** Averaging of en-face OCTA images improves the visualization of capillaries, particularly increasing the clarity of the FAZ borders, and therefore improves the correlation of vessel density and FAZ-specific parameters to DR severity and BCVA.

## Precis

Averaging of en-face SD-OCTA improves the visualization of capillaries compared to single images, and lower overall vessel length density is associated with worsening visual acuity and severity of diabetic retinopathy.

---

## INTRODUCTION

Despite being a preventable disease, diabetic retinopathy (DR) remains the leading cause of permanent vision loss in the working-age population.<sup>1</sup> The risk of blindness as well as the need for more aggressive treatment and close monitoring increases with the severity of DR.<sup>2</sup> Diabetic retinopathy is currently classified according to the International Clinical Diabetic Retinopathy Disease Severity Scale,<sup>3</sup> and capillary loss and macular non-perfusion have been shown to be significantly correlated with DR severity.<sup>4, 5</sup> Although the scale is well-defined, assigning the appropriate level of severity to a diabetic eye can be challenging. The primary diagnostic test to differentiate between non-proliferative and early proliferative diabetic retinopathy is fluorescein angiography (FA), a process that can identify microaneurysms, venous beading, capillary non-perfusion and leakage.<sup>6</sup> However, FA has several limitations including the inability to image the intermediate and deeper capillary networks,<sup>7</sup> a consequence of the limited depth resolution of FA as well as the innate properties of the fluorescein dye as it fills the superficial capillary plexus and blocks the visualization of the underlying plexuses. Additionally, patient discomfort due to intravenous injection, potential life-threatening allergic reactions,<sup>8, 9</sup> and long image acquisition times all contribute to difficulty with strict compliance to regular FA use.

In comparison to FA, optical coherence tomography angiography (OCTA) imaging has been shown to be a noninvasive, highly reproducible and repeatable method for quantifying the

vessel density (VD) measurements in healthy individuals and diabetics.<sup>10</sup> Recent studies using OCTA have also correlated capillary density loss and diabetic macular ischemia with worsening diabetic retinopathy severity and visual acuity.<sup>6, 11–18</sup> Even with advances in OCTA technology, image quality, reliability, and quantification are limited by patient fixation and artifacts including displacement, false positive and negative flow, gap defects, quilting defects, vessel doubling, white line artifacts and segmentation errors.<sup>19–21</sup> Recent studies have shown that averaging of multiple en-face OCTA images successfully enhances image quality and reduces discontinuous vessel segments, errors and background noise in both normal eyes<sup>22–25</sup> and diseased eyes affected by retinal vein occlusions (RVO),<sup>26</sup> diabetic microaneurysms,<sup>27</sup> and choroidal neovascularization.<sup>28</sup> The effect of en-face image averaging for identifying disease severity with different levels of diabetic retinopathy has not been reported to this date.

In this study, we averaged multiple OCTA images of both normal and diabetic eyes of varying stages of diabetic retinopathy without center-involved, clinically significant macular edema (CSME) to quantitatively compare retinal vascular features and correlate these metrics to best corrected visual acuity (BCVA) and DR severity. We then evaluated the efficacy of averaging compared to single OCTA images in terms of image quality and association with BCVA and DR severity.

## METHODS

This retrospective, cross-sectional cohort study received institutional review board (IRB) approval from Salus IRB (Austin, TX). This study complied with the Health Insurance Portability and Accountability Act of 1996 and followed the tenets of the Declaration of Helsinki. All individuals signed a written informed consent prior to participating in the study.

### Participants

One hundred and five eyes (65 patients) with 28 eyes from 19 healthy, aged-matched controls, 14 eyes from 9 diabetics without DR and 63 eyes from 37 diabetics with varying levels of DR without diabetic macular edema (DME), as indicated by their ongoing clinical care, were identified for the study from a vitreoretinal referral practice. Diabetics with varying levels of DR without DME and healthy, normal, age-matched controls without ocular or systemic diseases were imaged. Diabetic eyes with DME that would affect the quantitative metrics of the central 3×3 mm scan pattern were not included in this study due to potential segmentation errors which could impact OCTA measurements of the superficial retinal capillary layer (SRL) and deep retinal capillary layer (DRL). Eyes previously treated with non-central, focal laser therapy greater than 6 months prior were allowed to be included. Several of the included eyes were concurrently undergoing or had previous treatment with anti-vascular endothelial growth factor (anti-VEGF) injections including bevacizumab (Genentech, South San Francisco, CA, USA), aflibercept (Regeneron, Tarrytown, NJ, USA), or ranibizumab (Genentech, South San Francisco, CA, USA). All eyes, however, were well-controlled without signs of active DME or vitreous hemorrhage.

## Optical Coherence Tomography Imaging

All images were obtained consecutively in a single sitting and analyzed using a similar method as previously described.<sup>26</sup> In brief, all OCTA images were obtained using spectral-domain OCTA (Zeiss Cirrus 5000 with AngioPlex, Carl Zeiss Meditec, Inc., Dublin, CA) using the Angiography 3×3 mm scan pattern. Each OCTA scan consists of 245 A-scans at 245 B-scan positions, repeated 4 times at each location. En-face OCTA images were generated using the optical microangiography (OMAG<sup>®</sup>) algorithm. Images were centered on the fovea and standard OCTA tracking software was utilized to minimize motion artifacts. Scans were repeated to obtain 5 scans with signal strength between 7 out of a possible 10 to a full 10 out of 10, uniform illumination without areas of darkness, good foveal centration, and no significant evidence of motion artifact (evidenced by misalignment of vessel segments). Five structural B-scans were chosen as the optimal number of images for averaging based on our previous study.<sup>26</sup> Moreover, the findings from Uji and colleagues demonstrated that for the SRL, the largest difference in vessel length density (VLD) occurred in the first level of averaging and diminished in magnitude after five frames of averaging; and for the DRL, the ideal number of averaged images was more than three but no significant differences were found after 6 averaged images.<sup>25</sup> All images were reviewed, projection artifacts were removed using the Zeiss AngioPlex software (version 10.0; clearance by the US FDA pending, Carl Zeiss Meditec, Inc., Dublin, CA), and each segmentation was checked to ensure that the default segmentation boundaries of the device were correct in identifying the SRL and DRL, which were then exported at a size of 1024×1024 pixels for further analysis.

## Multiple En-Face Imaging Averaging

Utilizing the algorithm developed by Uji A et al., SRL and DRL en-face images were averaged using ImageJ (developed by Wayne Rasband, National Institutes of Health, Bethesda, MD; available at <http://rsb.info.nih.gov/ij/index.html>).<sup>25</sup> The corresponding structural B-scans were not averaged. An 819 × 819 pixels central square area was stacked to create a 5 frame video of the SRL images, followed by DRL images, and registered based on identifying fundus features. The resulting video was then averaged for both the SRL and DRL images and the corresponding averaged images were stitched together into a single averaged image.

## Quantitative Measurements

OCTA en-face images were exported and processed via the Zeiss AngioPlex algorithm (version 10.0; clearance by the US FDA pending, Carl Zeiss Meditec, Inc., Dublin, CA). Images were compared based on the size and circularity of the foveal avascular zone (FAZ), parafoveal VLD, and perfusion density (PD). These metrics were correlated with BCVA and the diabetic retinopathy severity score (DRSS) as assessed from clinical examination according to the International Clinical Diabetic Retinopathy Disease Severity Scale.

FAZ circularity is defined as the measure of the shape of the FAZ relative to a circle, with an abnormal FAZ circularity characterized by a lower value. VLD is defined as the total length of perfused vasculature per unit area ( $\text{mm}^{-1}$ ). PD is defined as the total area covered by perfused vasculature per unit area (%). Regions of measurement were based on the

parafoveal Early Treatment of Diabetic Retinopathy Study (ETDRS) subfields provided in the 3×3 mm OCTA scan pattern. VLD and PD measurements of the SRL and DRL were acquired for each ETDRS subfield and inner ring, which includes all of the parafoveal subfields.

Analyses were performed using the averaged image (average of the five acquisitions), as well as using a single image (the highest quality image with the highest signal strength), and the resultant metrics were compared.

### Statistical Analysis

Data was analyzed using the Stata 13.0 statistical package (StataCorp LP, College Station, TX, USA). All quantitative values were expressed as the mean with  $\pm$  standard deviation (SD). For continuous variables, including the FAZ-size and circularity, VLD of the SRL and DRL, and PD of the SRL and DRL of the normal age-matched control and DR eyes with varying levels of severity, an independent 2-tailed t-test was performed. For binary demographic variables, the Fisher exact test was performed. Univariate and stepwise multivariate linear regression with clustering on the individual level were performed to correlate quantitative metrics to DR severity. Statistical significance was defined as  $p < 0.05$ .

## RESULTS

### Demographics

There were 84 eyes of 55 patients including normal controls and varying levels of diabetic retinopathy who met the inclusion criteria. Twenty-eight eyes (19 patients) were healthy, age-matched controls; 11 eyes (8 patients) were diabetics without DR; 9 eyes (7 patients) had mild DR; 10 eyes (7 patients) had moderate DR; 5 eyes (3 patients) had severe DR; and 21 eyes (15 patients) had proliferative DR. The average hemoglobin A1C of the DR cohort was 7.0 ( $\pm 1.8$ ). Baseline characteristics of included subjects are summarized in Table 1. Comparing baseline demographic variables between the two cohorts, average age was 55.6 ( $\pm 16.4$ ) in the control group and 57.9 ( $\pm 11.4$ ) in the DR cohort ( $p=0.54$ , t-test). Laterality (42.9% right eyes in controls and 50% right eyes in DR,  $p=0.54$ ); gender (47.4% male in the control group and 66.7% in the DR group,  $p=0.17$ ); and lens status (96.4% phakic in controls and 89.3% phakic in DR,  $p=0.27$ ) were not significantly different as a proportion between the two groups. Mean logMAR BCVA was better in normal eyes ( $0.047 \pm 0.063$ , Snellen equivalent 20/22.5) when compared to DR eyes ( $0.081 \pm 0.090$ , Snellen equivalent 20/25, marginally significant at  $p=0.078$ ). At the time of image acquisition for the cross-sectional study, 9 eyes had been treated with anti-VEGF, 3 eyes with panretinal photocoagulation (PRP), 2 eyes with focal laser, 6 eyes with anti-VEGF and PRP, 3 eyes with anti-VEGF and focal laser, 1 eye with PRP and focal laser, and 2 eyes with anti-VEGF, PRP and focal laser.

### Single Versus Averaged Optical Coherence Tomography Angiography Images

Qualitative differences between averaged SRL and DRL (Figure 1, A and B) versus single (Figure 1, C and D) images after registration showed less vessel discontinuity in both averaged images of the SRL (Figure 1A) and the DRL (Figure 1B). Fewer artifactual flow

signals in non-vascular areas such as the FAZ, and smoother and more uniform capillaries in the SRL and DRL were evident in the averaged images. Similar findings were noted in eyes with diabetes without diabetic retinopathy with the averaged SRL (Figure 2A), DRL (Figure 2B) and FAZ (Figure 2C) versus single SRL (Figure 2D), DRL (Figure 2E), and FAZ (Figure 2F) with corresponding non-averaged structural B-scans of the SRL (Figure 2G), DRL (Figure 2H), and whole retina (Figure 2I); mild NPDR with the averaged SRL (Figure 3A), DRL (Figure 3B), and FAZ (Figure 3C) versus single SRL (Figure 3D), DRL (Figure 3E), and FAZ (Figure 3F) with corresponding non-averaged structural B-scans of the SRL (Figure 3G), DRL (Figure 3H), and whole retina (Figure 3I); moderate NPDR with the averaged SRL (Figure 4A), DRL (Figure 4B), FAZ (Figure 4C) versus single SRL (Figure 4D), DRL (Figure 4E), and FAZ (Figure 4F) with corresponding non-averaged structural B-scans of the SRL (Figure 4G), DRL (Figure 4H), and whole retina (Figure 4I); severe NPDR with the averaged SRL (Figure 5A), DRL (Figure 5B), and FAZ (Figure 5C) versus single SRL (Figure 5D), DRL (Figure 5E), and FAZ (Figure 5F) with corresponding non-averaged structural B-scans of the SRL (Figure 5G), DRL (Figure 5H), and whole retina (Figure 5I); and PDR with the averaged SRL (Figure 6A), DRL (Figure 6B), and FAZ (Figure 6C) versus single SRL (Figure 6D), DRL (Figure 6E), and FAZ (Figure 6F) with corresponding non-averaged structural B-scans of the SRL (Figure 6G), DRL (Figure 6H), and whole retina (Figure 6I).

Table 2 shows the univariate linear regression analysis comparing the quantitative metrics for both averaged and single images, including the VLD and PD measurements of both the SRL and DRL. Interestingly, FAZ size in averaged images was significantly larger than in single images among eyes with moderate non-proliferative diabetic retinopathy (NPDR) ( $0.39 \pm 0.17$  vs.  $0.23 \pm 0.14$ ,  $p = 0.034$ ) and proliferative DR ( $0.46 \pm 0.16$  vs.  $0.27 \pm 0.14$ ,  $p < 0.001$ ). In contrast, VLD and PD uniformly had significantly lower values in averaged images as compared to single images with the exception for a few parameters within each level of DR severity (Table 2). Control eyes and eyes with no DR measured significantly less in all SRL and DRL parameters in averaged images as compared to single images, as shown in Table 2.

Table 3 shows the univariate linear regression analysis comparing the quantitative metrics for both averaged and single images with BCVA. FAZ size was not associated with BCVA in single images ( $p = 0.31$ ), but was significantly associated in averaged images (coefficient 0.21,  $p = 0.004$ ). Similarly, for DRL temporal VLD, there was a significant association with BCVA in averaged images ( $-0.013$ ,  $p = 0.009$ ), but this did not reach statistical significance in single images ( $p = 0.058$ ). In contrast, SRL PD in inferior, nasal, and temporal regions in averaged images and DRL inferior PD (in either single or averaged images) were not significantly associated with BCVA. All other VLD and PD quantitative metrics examined (Table 3) were significantly associated with BCVA for both single images and averaged images (all  $p < 0.05$ ). All significantly associated VLD and PD factors had negative coefficients, which implies that a greater (more positive) value in the OCTA parameter is associated with a lower (better) logMAR BCVA. In contrast, in averaged images, increased FAZ size was associated with worse (greater logMAR value) BCVA.

Univariate linear regression analysis comparing the quantitative metrics for both averaged and single images with DR severity in Table 4 shows significant associations with DR severity in all SRL and DRL parameters ( $p < 0.05$ ) except in the SRL inferior PD. Similarly, FAZ circularity also had significant associations with DR severity in both averaged ( $-8.73$ ,  $p < 0.001$ ) and single images ( $-10.11$ ,  $p < 0.001$ ). FAZ size was the only factor that was significantly associated with DR severity in the univariate analysis of the averaged images ( $6.18$ ,  $p < 0.001$ ), but not in single images ( $p = 0.98$ ). All significantly associated VLD and PD factors demonstrated that an increased value was associated with less DR severity, whereas increased FAZ size and decreased FAZ circularity were both associated with worse DR severity.

When all OCTA parameters significantly associated with DR severity in the univariate analyses (Table 4, bolded  $p$ -values) were included in a multivariable linear regression model, averaging did not result in an increased  $R^2$  value ( $0.82$  and  $0.77$  for single and averaged groups, respectively). However, after including all the potential explanatory variables into the model, no variables remained significantly associated with DR severity in multivariate analysis with single images. By contrast, in averaged images, increased SRL superior ETDRS PD significantly predicted worse DR severity (coefficient  $52.7$ ,  $p=0.026$ ). A similar multivariate linear regression for the outcome of BCVA showed comparably low  $R^2$  values for both single ( $0.42$ ) and averaged ( $0.47$ ) images. However, after including all the potential explanatory variables into the model, increased DRL total PD on single image analysis was still significantly associated with worse BCVA ( $14.3$ ,  $p=0.018$ ). In averaged images, greater FAZ circularity in averaged images was still significantly associated with better BCVA ( $-2.81$ ,  $p=0.048$ ).

## DISCUSSION

We previously demonstrated that image averaging in RVO eyes showed improved visualization of angiographic en-face images. In this study, we evaluated the correlation between quantitative microvascular changes on spectral-domain OCTA with BCVA and severity of DR. Univariate analysis demonstrated that the correlation with BCVA was statistically significant for all quantitative variables except for FAZ size in the single images, and for the SRL inferior PD, SRL nasal PD, SRL temporal PD, and DRL inferior PD in the averaged images (Table 3). Similarly, DR severity was significantly correlated with all quantitative metrics except for the SRL inferior PD and FAZ size in the single images, and SRL inferior PD in the averaged images (Table 4). Multivariate analysis showed that after including all the potential explanatory variables into the model, no variables in single images remained significantly associated with DR severity, but increased SRL superior ETDRS PD in averaged images still significantly predicted worse DR severity. A similar multivariate linear regression for the outcome of BCVA showed that after including all the potential explanatory variables into the model, increased DRL total PD on single images was still significantly associated with worse BCVA, and that greater FAZ circularity in averaged images was still significantly associated with better BCVA.

We also demonstrated qualitative improvements with less discontinuous vessels, fewer artifactual flow signals in nonvascular areas such as the FAZ, and increased uniformity of

the capillary network when image averaging was used (Figures 1–6). Current limitations of quantitative analysis from OCTA include projection artifacts, discontinuous vessels, and decorrelation from eye motion artifacts that lead to false negative or positive appearance of flow. Recently, Holmen et al. found that the prevalence of artifacts associated with the reliability of quantitative values from commercially available OCTA may be as high as 53.5% in DR.<sup>20</sup> In addition, OCTA is an acquired image that has a certain threshold of imaging capabilities that may not capture the flow signal in a region of interest. This, compounded by the natural cardiac cycle and pulsatile nature of blood flow, may lead to slight variations in the repeatability of quantitative metrics from a single image.<sup>19</sup> Recently, Kaizu Y and colleagues demonstrated increased microaneurysm detection with image averaging, which captured subtle flow particularly in focal bulge-type microaneurysms with more averaged frames.<sup>27</sup> Image averaging has been shown to limit movement artifacts and improve the continuity of vascular structures, which reduces irregular vessel segments, noise, and discontinuities<sup>22, 24–28</sup> and would all contribute to overall lower quantitative vessel density measurements.<sup>22, 24–26</sup> This benefit of image averaging is illustrated for eyes with all levels of diabetic severity (Figures 1–6).

Compared to conventional FA, OCTA is a relatively easily acquired, non-invasive imaging technique that allows for depth-resolved mapping of the retinal and inner choroidal vasculature.<sup>29–31</sup> Averaging improves the qualitative and quantitative metrics in both healthy<sup>22, 25</sup> and diseased eyes,<sup>26, 27</sup> and this may improve the repeatability, reproducibility and reliability of these values. Image averaging, however, is not without its challenges. The acquisition of 5 high quality images in diseased eyes requires that several factors be addressed, including increased acquisition time associated with limitations in acquisition speed with the spectral-domain OCTA,<sup>24, 26</sup> automated segmentation errors,<sup>17, 21</sup> patient comfort, and poor fixation. All images included in our study did not have CSME and had 7 signal strength, proper centration, and adequate focus as these variables have been shown to affect the reproducibility of quantitative OCTA metrics.<sup>14, 20, 32, 33</sup> Uji and colleagues demonstrated that the largest improvement with averaging of the SRL occurred after 2 images and had diminished returns after 5 frames. Similarly, in the DRL, the ideal number of frames was more than 3 but less than 6.<sup>23</sup> Optimizing the number of averaged images for each capillary plexus and improving the acquisition speed with higher frequency spectral-domain or swept-source OCTA devices may improve our ability to reproduce high quality and reliable quantitative measurements.

Similar to previous reports, we demonstrated that the severity of diabetic retinopathy correlated with quantitative metrics.<sup>12–16, 18, 34–39</sup> Both single and averaged images showed a significant correlation ( $R^2 = 0.77$  [Averaged] vs 0.82 [Single]) with DR severity when optimizing all available predictive OCTA quantitative metrics. In terms of univariate regression, diabetic retinopathy severity was significantly correlated with all quantitative metrics except for the SRL inferior PD and FAZ size in the single images, and SRL inferior PD in the averaged images (Table 4). Consistent with prior studies, the areas of capillary non-perfusion within the perifoveal intercapillary areas in averaged images increased in a statistically significant manner with the severity of DR.<sup>12–16, 18, 34–39</sup> Current commercial software more readily measure SRL quantitative microvascular changes on OCTA and therefore have been used previously to differentiate healthy eyes from DR eyes.<sup>13, 14</sup>



However, it is clear that DRL ischemia also correlates with DR severity<sup>16, 38, 39</sup> and BCVA.<sup>11</sup> Reliable and reproducible DRL measurements are difficult to obtain due to projection artifacts.<sup>13, 19</sup> In our study, we were able to better qualitatively delineate the SRL and DRL (Figures 1–6) by removing projection artifacts and increasing our sampling density with averaging 5 images. Consequently, all DRL quantitative VLD and PD values were significantly associated with DR severity in both single and averaged images and contributed to the high  $R^2$  values. In addition, averaged image analysis of FAZ size measurements were noted to be larger as compared to single images among eyes with moderate NPDR (0.39 [ $\pm 0.17$ ] vs. 0.23 [ $\pm 0.14$ ]  $p = 0.034$ ) and proliferative DR (0.46 [ $\pm 0.16$ ] vs. 0.27 [ $\pm 0.14$ ]  $p < 0.001$ ). This is likely due to less artifactual flow signals and improved signal to noise ratio within the FAZ in averaged images. Similar to the findings from Uji et al.<sup>22, 25</sup> and our previous report with RVO,<sup>26</sup> all VLD and PD quantitative metrics demonstrated lower values on averaged images compared to single images across all cohorts including control eyes (Table 2). These findings are likely due to the less vessel discontinuity and artefactual spines in the averaged images compared to the single images. Our study demonstrated that future software algorithms utilizing both averaged SRL and DRL metrics may allow for a more accurate correlation to DR severity.

Quantitative OCTA metric parameters used to assess the retinal microvasculature may be useful to monitor functional visual impairment in diabetic eyes. Although not as robust as the correlation with DR severity, the correlation in the multivariate analysis for BCVA ( $R^2 = 0.54$  [Averaged] vs 0.42 [Single]) was still associated with loss of SRL and DRL perifoveal capillary vasculature. Interestingly, FAZ size for the averaged images was predictive of worse BCVA but not with the single images; and foveal avascular zone circularity also correlated with worse BCVA. Previous studies have also showed a similarly mild correlation of FAZ parameters with visual acuity in both DR and RVO.<sup>6, 11, 26, 40</sup> Observations that may explain the weaker correlations between FAZ parameters and BCVA include difficulty interpreting and delineating the FAZ in diabetic eyes, given the enlarging FAZ zones with worsening DR severity and the natural variability within healthy individuals.<sup>13, 16, 41</sup> We demonstrated that, as compared to single images, image averaging improves the visualization of vessels, particularly increasing clarity at the FAZ borders, which resulted in improvement of the correlation of FAZ-specific parameters (such as size and circularity) to DR severity and BCVA, and also therefore increased the overall reliability of these quantitative metrics predicting visual outcomes.

Mean vessel density especially in the deep capillary plexus has been shown to be lower in diabetic eyes with increasing disease severity<sup>18</sup> and the loss is greater in eyes with decreased visual acuity.<sup>11</sup> Interestingly, Sim and colleagues<sup>42</sup> only found a 15% correlation of macular ischemia with visual function in eyes with moderate to severe macular ischemia on fluorescein angiography. Similarly, Samara and colleagues demonstrated only a modest correlation between the superficial network ( $R^2 = 0.29$ ,  $p < 0.01$ ) and deep network ( $R^2 = 0.48$ ,  $p < 0.001$ ) vessel density measurements with BCVA.<sup>6</sup> In the present study, even with image averaging, we also noted a similar modest correlation with BCVA ( $R^2 = 0.54$  [Averaged] and 0.42 [Single]). These findings may indicate that even with continued loss of capillary vessels within the deep capillary plexus (DCP), BCVA may be maintained until a threshold is reached beyond which normal vision will deteriorate.<sup>6, 11</sup> Studies have shown

that the DCP is more susceptible to ischemia due to it being the watershed zone and terminal units of the capillary plexus.<sup>43</sup> In our multivariate analysis, both SRL and DRL quantitative metrics were significantly associated with BCVA. Although the decrease in vessel density may be observed in both plexuses, a moderate loss of capillary perfusion may still be compatible with normal vision but cause subtle losses in contrast sensitivity, electroretinographic changes, and color vision.<sup>44</sup> Further longitudinal studies are warranted to identify the threshold of capillary nonperfusion at which these visual functions are affected.

This study provides important information about the ability to analyze quantitative metrics in averaged versus single OCTA images in eyes with different stages of DR severity. We acknowledge the study's limited sample size with relatively small number of eyes in each stage of DR, its cross-sectional design, and the limitations of utilizing only the Zeiss AngioPlex spectral-domain OCTA system, and that the results may not be reproducible across other commercial platforms. Adjusted automated segmentation boundaries in the diseased eyes could lead to segmentation errors especially in the DRL as, even with the projection artifacts removed, the superficial vessels may still affect the quantitative metrics analysis. We attempted to minimize the amount of segmentation errors by requiring high quality, focused images with strong signal strength and excluding eyes with center-involved DME. Lastly, several eyes were previously treated with a combination of anti-VEGF, laser, or both modalities and these treatments may affect quantitative measurements, although previous studies have shown that PRP<sup>45</sup> and anti-VEGF<sup>46, 47</sup> do not affect macular perfusion. Further larger, longitudinal studies with well-defined treatment naïve groups with each level of DR severity adjusted for systemic risk factors (such as duration of diabetes, hemoglobin A1C, cardiovascular disease, hypertension, smoking history, and hyperlipidemia; and demographic factors such as age and sex) may be able to delineate the benefits of image averaging of multiple frames in reducing qualitative artifacts and improving the predictive nature of quantitative OCTA metrics.

Despite these limitations, our study is the first to demonstrate the qualitative and quantitative improvement with registered image averaging in eyes with varying degrees of DR severity. Given the observation that proliferative retinopathy and diabetic macular edema are more common in eyes with poorer microvascular perfusion and increased leakage,<sup>39, 48</sup> these eyes may be at risk for rapidly progressive disease, and thus earlier identification of eyes at significant risk due to lower vascular density and macular ischemia may provide for better individualized management of diabetic retinal disease. In conclusion, visualization of vessels in OCTA images improves with averaging, and both single and averaged imaged quantitative biomarkers correlate to DR severity and BCVA. Utilizing en-face OCTA image averaging may improve the reproducibility and reliability of OCTA technology when identifying the presence and monitoring the progression of macular ischemia in diabetic retinopathy.

### Financial Support:

This work was supported in part by an unrestricted grant from Research to Prevent Blindness (RPB) and Career Development Awards from Research to Prevent Blindness (QVH) and K08 Grant (QVH, 1 K08 EY023595, National Eye Institute, NIH). The sponsor or funding organization had no role in the design or conduct of this research.

## Abbreviations/Acronyms:

<b>anti-VEGF</b>	Anti-Vascular Endothelial Growth Factor
<b>BCVA</b>	Best correct visual acuity
<b>DRL</b>	Deep retinal layer
<b>DR</b>	Diabetic Retinopathy
<b>DRSS</b>	Diabetic retinopathy severity score
<b>ETDRS</b>	Early Treatment of Diabetic Retinopathy Study
<b>FAZ</b>	Foveal avascular zone
<b>FA</b>	Fluorescein angiography
<b>IRB</b>	Institutional review board
<b>logMAR</b>	Logarithm of the minimum angle of resolution
<b>NPDR</b>	Non-proliferative diabetic retinopathy
<b>OCTA</b>	Optical coherence tomography angiography
<b>OMAG<sup>®</sup></b>	Optical microangiography
<b>PRP</b>	Panretinal photocoagulation
<b>PD</b>	Perfusion density
<b>RVO</b>	Retinal vein occlusions
<b>SRL</b>	Superficial retinal layer
<b>VLD</b>	Vessel length density

## REFERENCES

1. Nentwich MM, Ulbig MW. Diabetic retinopathy - ocular complications of diabetes mellitus. *World J Diabetes* 2015;6(3):489–99. [PubMed: 25897358]
2. Lee R, Wong TY, Sabanayagam C. Epidemiology of diabetic retinopathy, diabetic macular edema and related vision loss. *Eye Vis (Lond)* 2015;2:17. [PubMed: 26605370]
3. Wilkinson CP, Ferris FL 3rd, Klein RE, et al. Proposed international clinical diabetic retinopathy and diabetic macular edema disease severity scales. *Ophthalmology* 2003;110(9):1677–82. [PubMed: 13129861]
4. Fluorescein angiographic risk factors for progression of diabetic retinopathy. ETDRS report number 13. Early Treatment Diabetic Retinopathy Study Research Group. *Ophthalmology* 1991;98(5 Suppl):834–40. [PubMed: 2062516]
5. Reddy RK, Pieramici DJ, Gune S, et al. Efficacy of Ranibizumab in Eyes with Diabetic Macular Edema and Macular Nonperfusion in RIDE and RISE. *Ophthalmology* 2018;125(10):1568–74. [PubMed: 29752001]
6. Samara WA, Shahladee A, Adam MK, et al. Quantification of Diabetic Macular Ischemia Using Optical Coherence Tomography Angiography and Its Relationship with Visual Acuity. *Ophthalmology* 2017;124(2):235–44. [PubMed: 27887743]

7. Spaide RF, Klancnik JM Jr., Cooney MJ. Retinal vascular layers imaged by fluorescein angiography and optical coherence tomography angiography. *JAMA Ophthalmol* 2015;133(1):45–50. [PubMed: 25317632]
8. Yannuzzi LA, Rohrer KT, Tindel LJ, et al. Fluorescein angiography complication survey. *Ophthalmology* 1986;93(5):611–7. [PubMed: 3523356]
9. Karhunen U, Raitta C, Kala R. Adverse reactions to fluorescein angiography. *Acta Ophthalmol (Copenh)* 1986;64(3):282–6. [PubMed: 2944349]
10. Lei J, Durbin MK, Shi Y, et al. Repeatability and Reproducibility of Superficial Macular Retinal Vessel Density Measurements Using Optical Coherence Tomography Angiography En Face Images. *JAMA Ophthalmol* 2017;135(10):1092–8. [PubMed: 28910435]
11. Dupas B, Minvielle W, Bonnin S, et al. Association Between Vessel Density and Visual Acuity in Patients With Diabetic Retinopathy and Poorly Controlled Type 1 Diabetes. *JAMA Ophthalmol* 2018;136(7):721–8. [PubMed: 29800967]
12. Ting DSW, Tan GSW, Agrawal R, et al. Optical Coherence Tomographic Angiography in Type 2 Diabetes and Diabetic Retinopathy. *JAMA Ophthalmol* 2017;135(4):306–12. [PubMed: 28208170]
13. Durbin MK, An L, Shemonski ND, et al. Quantification of Retinal Microvascular Density in Optical Coherence Tomographic Angiography Images in Diabetic Retinopathy. *JAMA Ophthalmol* 2017;135(4):370–6. [PubMed: 28301651]
14. Kim AY, Chu Z, Shahidzadeh A, et al. Quantifying Microvascular Density and Morphology in Diabetic Retinopathy Using Spectral-Domain Optical Coherence Tomography Angiography. *Invest Ophthalmol Vis Sci* 2016;57(9):OCT362–70. [PubMed: 27409494]
15. Alibhai AY, De Pretto LR, Moulton EM, et al. Quantification of Retinal Capillary Nonperfusion in Diabetics Using Wide-Field Optical Coherence Tomography Angiography. *Retina* 2018.
16. Hwang TS, Gao SS, Liu L, et al. Automated Quantification of Capillary Nonperfusion Using Optical Coherence Tomography Angiography in Diabetic Retinopathy. *JAMA Ophthalmol* 2016;134(4):367–73. [PubMed: 26795548]
17. Schottenhamml J, Moulton EM, Ploner S, et al. An Automatic, Intercapillary Area-Based Algorithm for Quantifying Diabetes-Related Capillary Dropout Using Optical Coherence Tomography Angiography. *Retina* 2016;36 Suppl 1:S93–S101. [PubMed: 28005667]
18. Nesper PL, Roberts PK, Onishi AC, et al. Quantifying Microvascular Abnormalities With Increasing Severity of Diabetic Retinopathy Using Optical Coherence Tomography Angiography. *Invest Ophthalmol Vis Sci* 2017;58(6):BIO307–BIO15. [PubMed: 29059262]
19. Spaide RF, Fujimoto JG, Waheed NK. Image Artifacts in Optical Coherence Tomography Angiography. *Retina* 2015;35(11):2163–80. [PubMed: 26428607]
20. Holmen IC, Konda MS, Pak JW, et al. Prevalence and Severity of Artifacts in Optical Coherence Tomographic Angiograms. *JAMA Ophthalmol* 2019.
21. Spaide RF, Fujimoto JG, Waheed NK, et al. Optical coherence tomography angiography. *Prog Retin Eye Res* 2018;64:1–55. [PubMed: 29229445]
22. Uji A, Balasubramanian S, Lei J, et al. Choriocapillaris Imaging Using Multiple En Face Optical Coherence Tomography Angiography Image Averaging. *JAMA Ophthalmol* 2017;135(11):1197–204. [PubMed: 28983552]
23. Arya M, Rebhun CB, Alibhai AY, et al. Parafoveal Retinal Vessel Density Assessment by Optical Coherence Tomography Angiography in Healthy Eyes. *Ophthalmic Surg Lasers Imaging Retina* 2018;49(10):S5–S17.
24. Lauermaann JL, Xu Y, Heiduschka P, et al. Impact of integrated multiple image averaging on OCT angiography image quality and quantitative parameters. *Graefes Arch Clin Exp Ophthalmol* 2019.
25. Uji A, Balasubramanian S, Lei J, et al. Impact of Multiple En Face Image Averaging on Quantitative Assessment from Optical Coherence Tomography Angiography Images. *Ophthalmology* 2017;124(7):944–52. [PubMed: 28318637]
26. Jung JJ, Chen MH, Shi Y, et al. Correlation of En Face Optical Coherence Tomography Angiography Averaging Versus Single-Image Quantitative Measurements with Retinal Vein Occlusion Visual Outcomes. *Retina* 2019.

27. Kaizu Y, Nakao S, Wada I, et al. Microaneurysm Imaging Using Multiple En Face OCT Angiography Image Averaging: Morphology and Visualization. *Ophthalmol Retina* 2020;4(2):175–86. [PubMed: 31753811]
28. Murakawa S, Maruko I, Kawano T, et al. Choroidal neovascularization imaging using multiple en face optical coherence tomography angiography image averaging. *Graefes Arch Clin Exp Ophthalmol* 2019;257(6):1119–25. [PubMed: 30783783]
29. Jia Y, Tan O, Tokayer J, et al. Split-spectrum amplitude-decorrelation angiography with optical coherence tomography. *Opt Express* 2012;20(4):4710–25. [PubMed: 22418228]
30. Schwartz DM, Fingler J, Kim DY, et al. Phase-variance optical coherence tomography: a technique for noninvasive angiography. *Ophthalmology* 2014;121(1):180–7. [PubMed: 24156929]
31. Borrelli E, Sadda SR, Uji A, Querques G. Pearls and Pitfalls of Optical Coherence Tomography Angiography Imaging: A Review. *Ophthalmol Ther* 2019;8(2):215–26. [PubMed: 30868418]
32. Lim HB, Kim YW, Kim JM, et al. The Importance of Signal Strength in Quantitative Assessment of Retinal Vessel Density Using Optical Coherence Tomography Angiography. *Sci Rep* 2018;8(1):12897. [PubMed: 30150636]
33. Tomlinson A, Hasan B, Lujan BJ. Importance of Focus in OCT Angiography. *Ophthalmol Retina* 2018;2(7):748–9. [PubMed: 31047385]
34. Salz DA, de Carlo TE, Adhi M, et al. Select Features of Diabetic Retinopathy on Swept-Source Optical Coherence Tomographic Angiography Compared With Fluorescein Angiography and Normal Eyes. *JAMA Ophthalmol* 2016;134(6):644–50. [PubMed: 27055248]
35. Carnevali A, Sacconi R, Corbelli E, et al. Optical coherence tomography angiography analysis of retinal vascular plexuses and choriocapillaris in patients with type 1 diabetes without diabetic retinopathy. *Acta Diabetol* 2017;54(7):695–702. [PubMed: 28474119]
36. Vujosevic S, Toma C, Villani E, et al. Early Detection of Microvascular Changes in Patients with Diabetes Mellitus without and with Diabetic Retinopathy: Comparison between Different Swept-Source OCT-A Instruments. *J Diabetes Res* 2019;2019:2547216. [PubMed: 31281849]
37. de Carlo TE, Chin AT, Bonini Filho MA, et al. Detection of Microvascular Changes in Eyes of Patients with Diabetes but Not Clinical Diabetic Retinopathy Using Optical Coherence Tomography Angiography. *Retina* 2015;35(11):2364–70. [PubMed: 26469537]
38. Agemy SA, Scripsema NK, Shah CM, et al. Retinal Vascular Perfusion Density Mapping Using Optical Coherence Tomography Angiography in Normals and Diabetic Retinopathy Patients. *Retina* 2015;35(11):2353–63. [PubMed: 26465617]
39. Sun Z, Tang F, Wong R, et al. OCT Angiography Metrics Predict Progression of Diabetic Retinopathy and Development of Diabetic Macular Edema: A Prospective Study. *Ophthalmology* 2019;126(12):1675–84. [PubMed: 31358386]
40. Balaratnasingam C, Inoue M, Ahn S, et al. Visual Acuity Is Correlated with the Area of the Foveal Avascular Zone in Diabetic Retinopathy and Retinal Vein Occlusion. *Ophthalmology* 2016;123(11):2352–67. [PubMed: 27523615]
41. Arend O, Wolf S, Harris A, Reim M. The relationship of macular microcirculation to visual acuity in diabetic patients. *Arch Ophthalmol* 1995;113(5):610–4. [PubMed: 7748131]
42. Sim DA, Keane PA, Zarranz-Ventura J, et al. The effects of macular ischemia on visual acuity in diabetic retinopathy. *Invest Ophthalmol Vis Sci* 2013;54(3):2353–60. [PubMed: 23449720]
43. Garrity ST, Paques M, Gaudric A, et al. Considerations in the Understanding of Venous Outflow in the Retinal Capillary Plexus. *Retina* 2017;37(10):1809–12. [PubMed: 28737534]
44. Tzekov R, Arden GB. The electroretinogram in diabetic retinopathy. *Surv Ophthalmol* 1999;44(1):53–60. [PubMed: 10466588]
45. Lorusso M, Milano V, Nikolopoulou E, et al. Panretinal Photocoagulation Does Not Change Macular Perfusion in Eyes With Proliferative Diabetic Retinopathy. *Ophthalmic Surg Lasers Imaging Retina* 2019;50(3):174–8. [PubMed: 30893451]
46. Couturier A, Rey PA, Erginay A, et al. Widefield OCT-Angiography and Fluorescein Angiography Assessments of Nonperfusion in Diabetic Retinopathy and Edema Treated with Anti-Vascular Endothelial Growth Factor. *Ophthalmology* 2019;126(12):1685–94. [PubMed: 31383483]
47. Ghasemi Falavarjani K, Iafe NA, Hubschman JP, et al. Optical Coherence Tomography Angiography Analysis of the Foveal Avascular Zone and Macular Vessel Density After Anti-

- VEGF Therapy in Eyes With Diabetic Macular Edema and Retinal Vein Occlusion. *Invest Ophthalmol Vis Sci* 2017;58(1):30–4. [PubMed: 28114569]
48. Vieira-Potter VJ, Karamichos D, Lee DJ. Ocular Complications of Diabetes and Therapeutic Approaches. *Biomed Res Int* 2016;2016:3801570. [PubMed: 27119078]

Author Manuscript

Author Manuscript

Author Manuscript

Author Manuscript

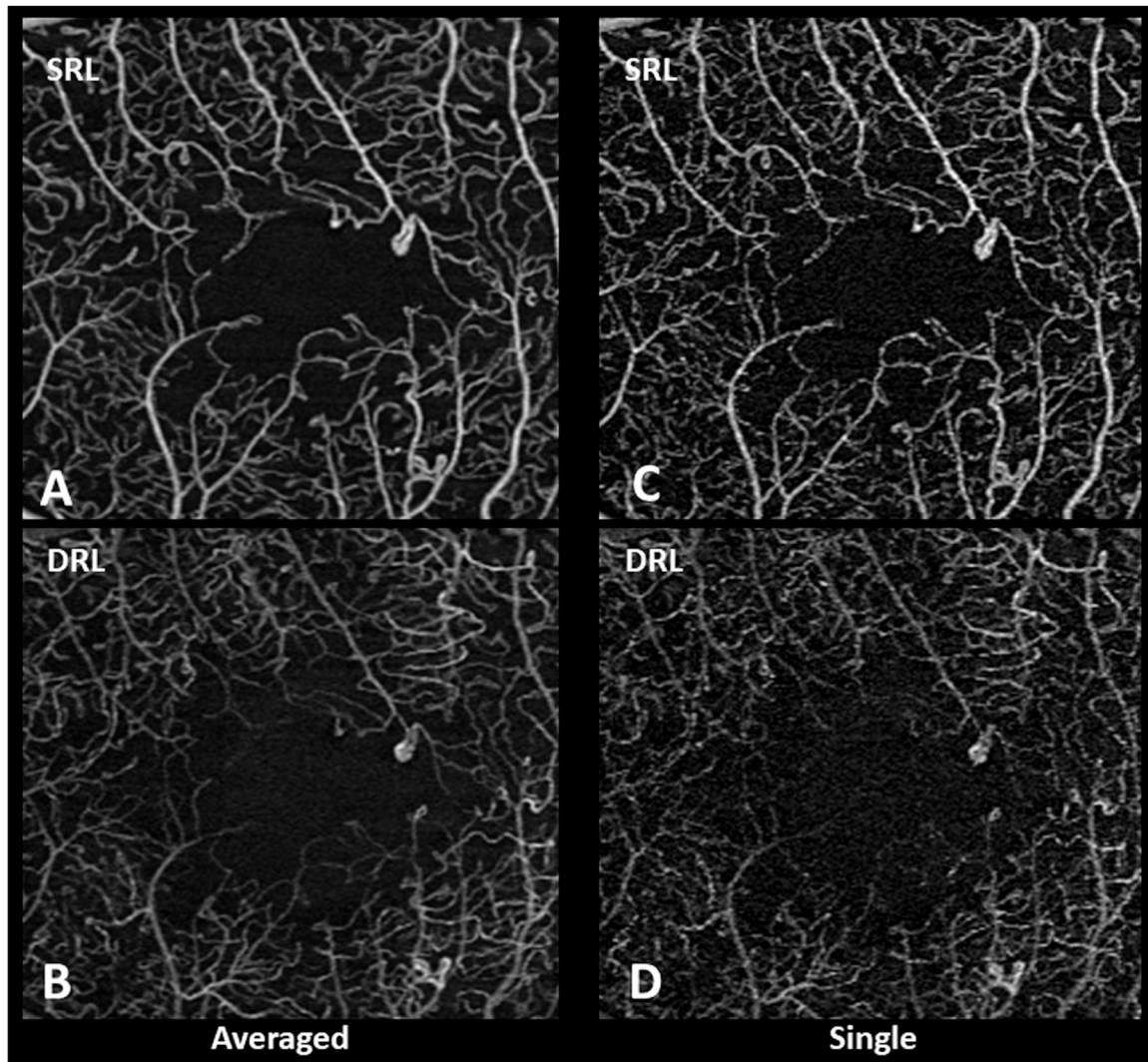


**Figure 1.** Qualitative differences between averaged and single spectral-domain optical coherence tomography angiography images of the superficial retinal layer (SRL) and deep retinal layer (DRL). Averaged SRL (A) and DRL (B) show fewer movement artifacts and background noise with better continuity of microvasculature compared to single SRL (C) and DRL (D).

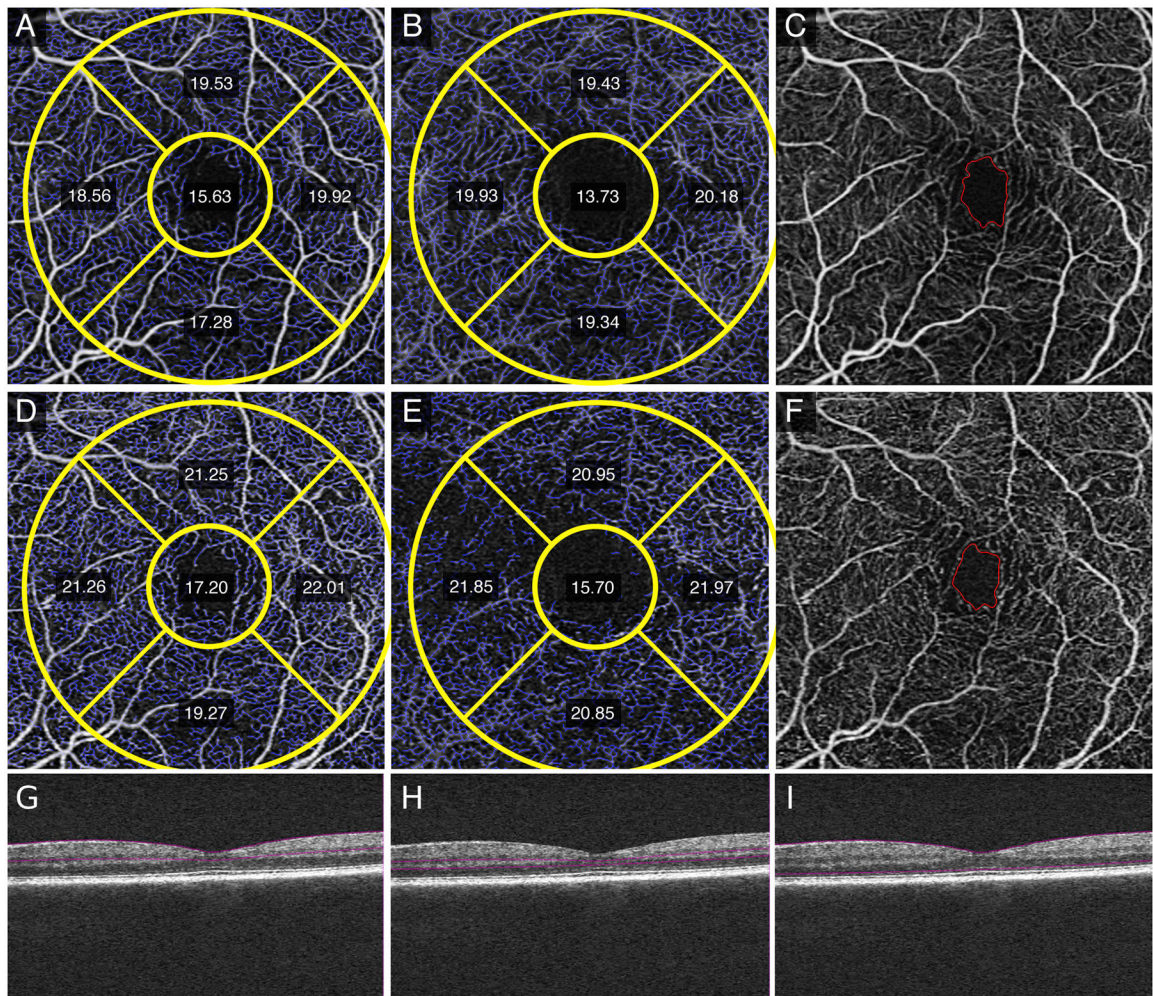


**Figure 2.** Quantitative measurements of vessel length density (VLD) in the parafoveal Early Treatment Diabetic Retinopathy Study (ETDRS) subfields, foveal avascular zone (FAZ) size, and FAZ circularity of a left eye with no clinical diabetic retinopathy. Averaged SRL (A) and DRL (B) show decreased VLD measurements and FAZ size (C) compared to single SRL (D), DRL (E) and FAZ size (F) images. Structural non-averaged B-scans show the segmentation for the SRL (G), DRL (H), and full retina (I).



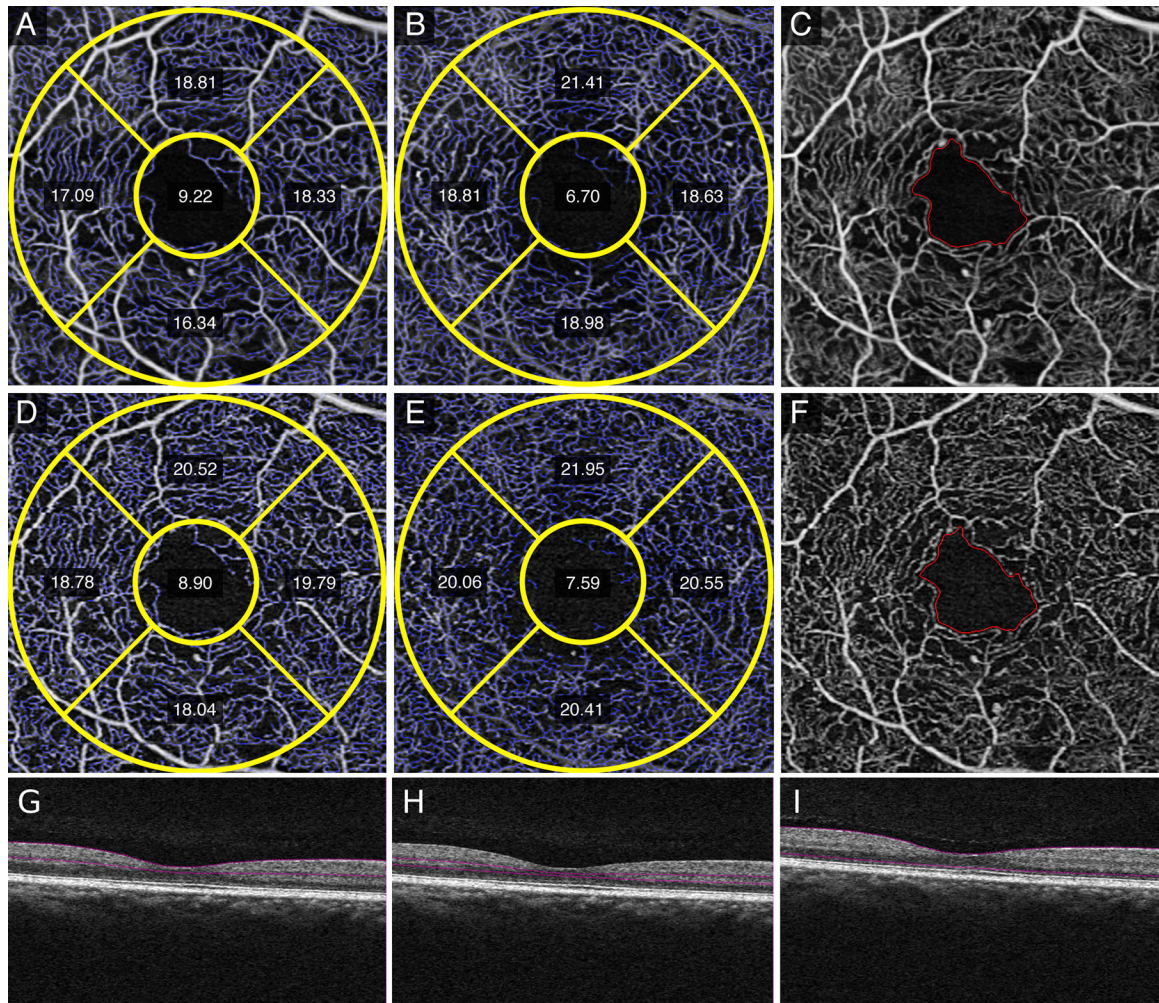


**Figure 3.** Quantitative measurements of vessel length density (VLD) in the parafoveal Early Treatment Diabetic Retinopathy Study (ETDRS) subfields, foveal avascular zone (FAZ) size, and FAZ circularity of a right eye with mild non-proliferative diabetic retinopathy. Averaged superficial retinal layer (SRL) (A) and deep retinal layer (DRL) (B) show decreased inferior and nasal VLD measurements in both the SRL and DRL, respectively and improved image quality in terms of vessel continuity around the FAZ (C) compared to single SRL (D), DRL (E), and FAZ (F) images. Structural non-averaged B-scans show the segmentation for the SRL (G), DRL (H), and full retina (I).

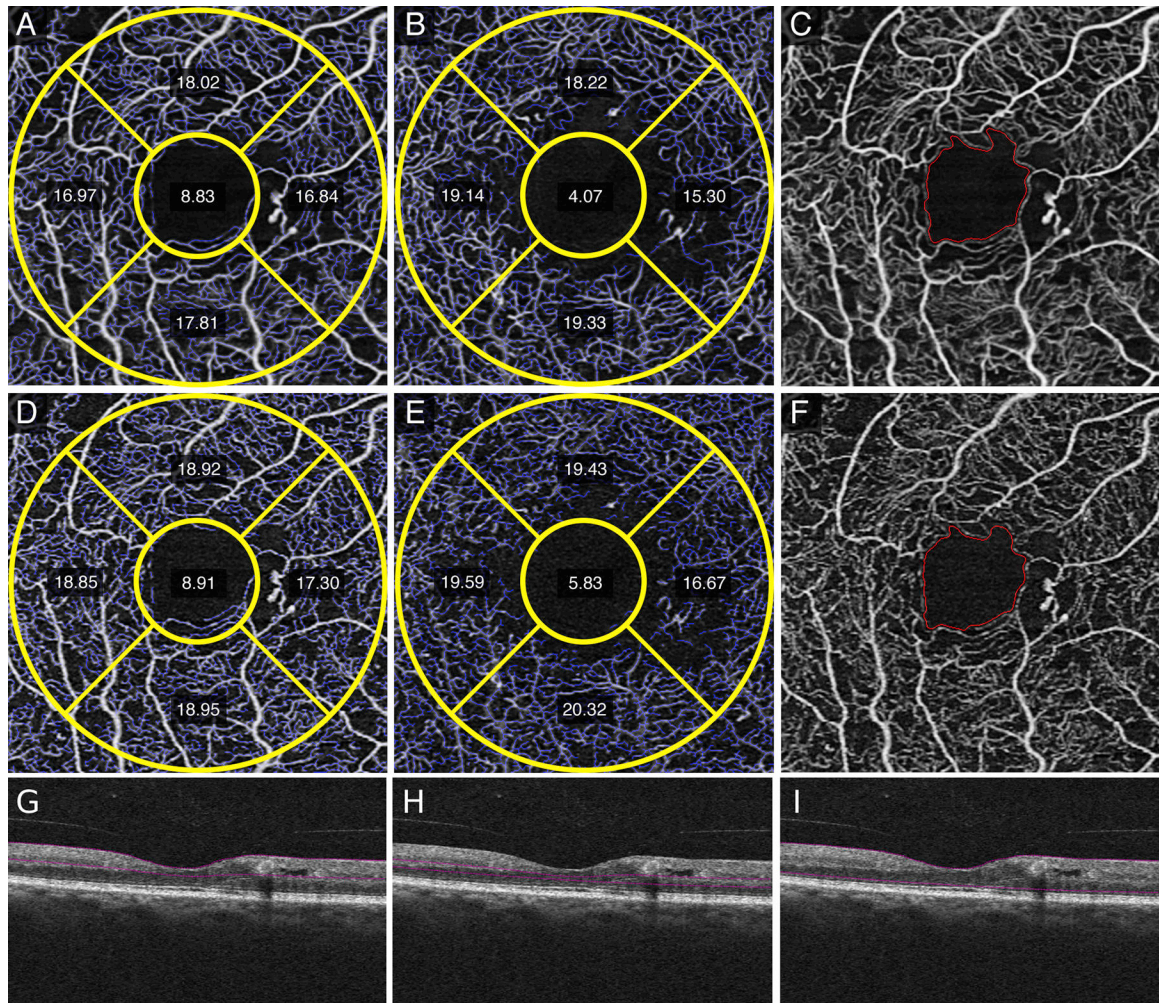


**Figure 4.** Qualitative and quantitative differences between averaged superficial retinal layer (SRL) (A), deep retinal layer (DRL) (B), and foveal avascular zone (FAZ) compared to single image SRL (D), DRL (E), and FAZ (F) show decreased vessel length density (VLD) measurements in the inferior and nasal subfields of a right eye with moderate non-proliferative diabetic retinopathy. Decreased background noise and better vessel continuity is seen in averaged (A,B, C) images compared to single images (D, E, F). The corresponding, non-averaged B-scan demonstrates the segmentation for the SRL (G), DRL (H), and full retina (I).

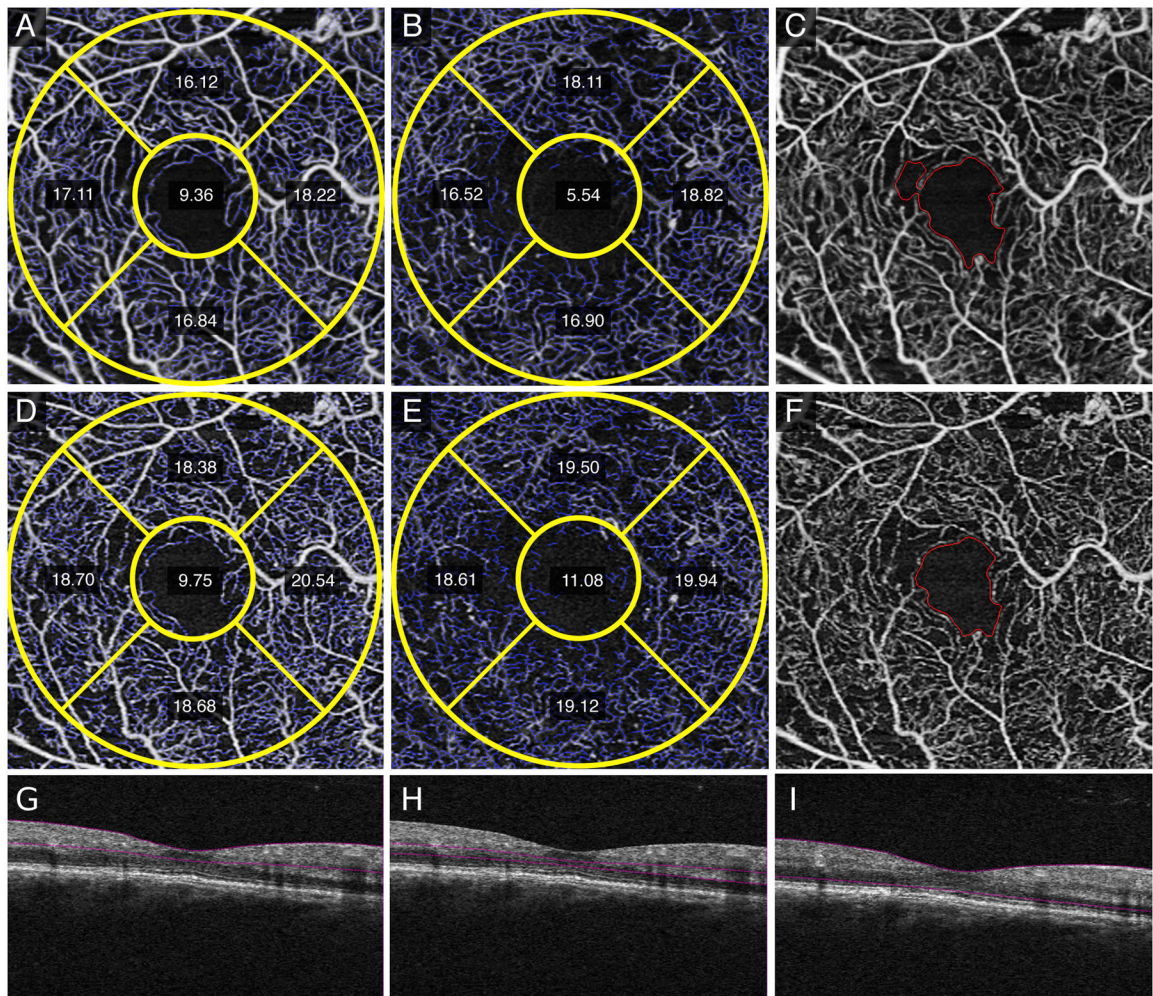


**Figure 5.**

In a right eye with severe non-proliferative diabetic retinopathy, averaged superficial retinal layer (SRL) (A), deep retinal layer (DRL) (B), and fundus images with foveal avascular zone (FAZ) delineated (C) versus single image SRL (D), DRL (E), and FAZ (F) images show decreased vessel length density (VLD) measurements, improved vessel structure, and decreased noise, respectively. The structural non-averaged B-scans show the segmentation for the SRL (G), DRL (H), and full retina (I).

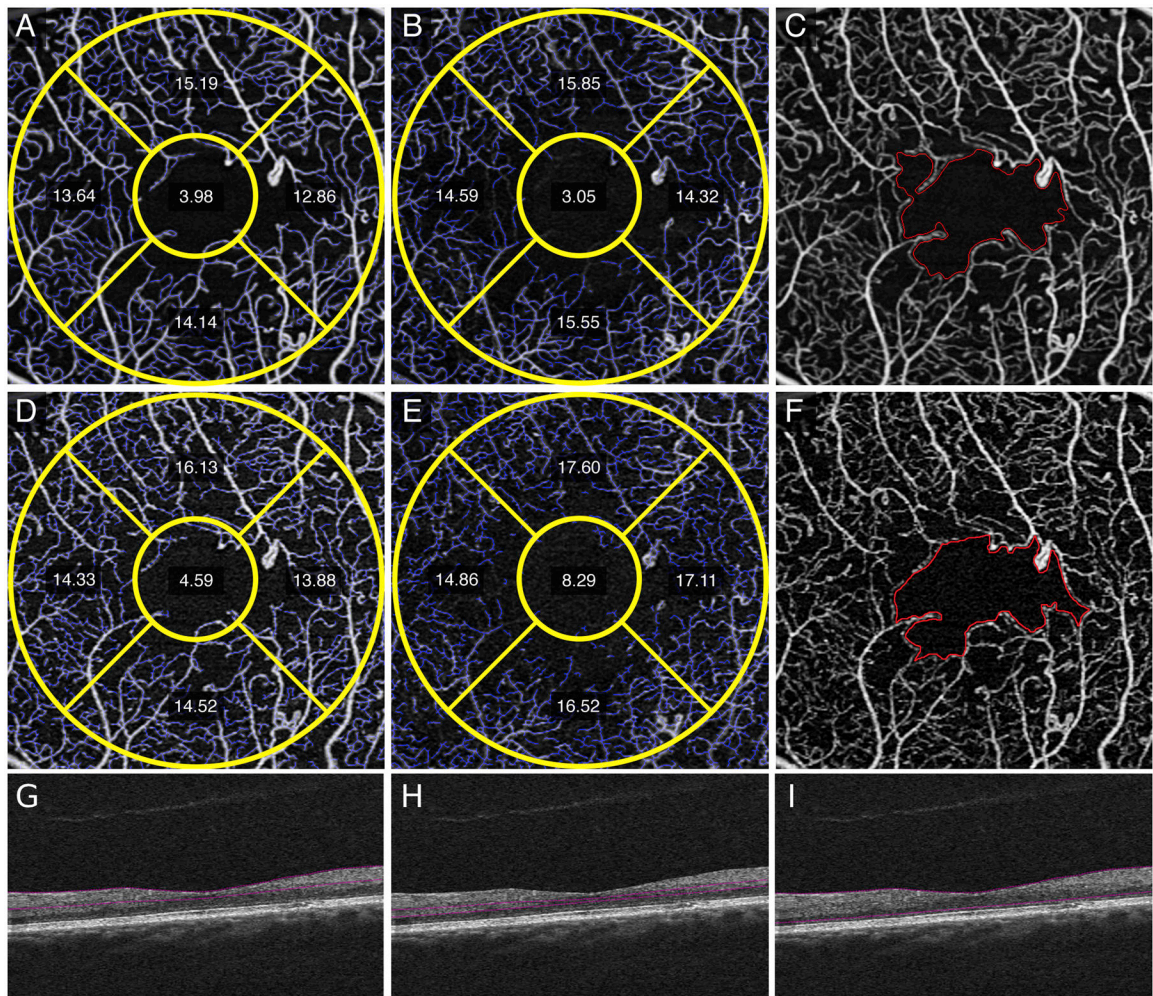


**Figure 6.**

Images of a left eye with proliferative diabetic retinopathy shows quantitative differences between averaged versus single images. Measurements in the averaged superficial retinal layer (SRL) (A), deep retinal layer (DRL) (B) and foveal avascular zone (FAZ) (C) images show decrease in FAZ size and vessel length density (VLD) measurements compared to the single SRL (D), DRL (E), and FAZ (F) images. FAZ abnormality is better visualized in averaged fundus (C) versus single fundus image (F) due to decrease in noise and improved vessel continuity. Structural non-averaged B-scans demonstrate the corresponding segmentation for the SRL (G), DRL (H), and full retina (I).

**Table 1.**

## Demographics

Variables	Age-Matched Controls N=28 eyes from 19 subjects	Eyes with Diabetes N=56 eyes from 36 subjects	P-Value
Age	55.6 ( $\pm$ 16.4)	57.9 ( $\pm$ 11.4)	0.54
Laterality (Right Eye)	12 (42.9%)	28 (50.0%)	0.54
Gender (Male)	9 (47.4%)	24 (66.7%)	0.17
Lens Status (Phakic)	27 (96.4%)	50 (89.3%)	0.27
LogMAR BCVA	0.047 ( $\pm$ 0.063)	0.081 ( $\pm$ 0.090)	0.078
Hgb A1C		7.0 ( $\pm$ 1.8)	

Baseline demographics comparing control eyes to eyes with diabetes. LogMAR BCVA = logarithm of the minimum angle of resolution best corrected visual acuity. Hgb = hemoglobin.

Table 2.

Univariate Analysis of Quantitative Metrics in Averaged and Single Images

Variable	Control			Mild			Moderate			Severe			Proliferative		
	(SD) Averaged Images	(SD) Single Images	P	Mild DR (SD) Averaged Images	Mild DR (SD) Single Images	P	Moderate DR (SD) Averaged Images	Moderate DR (SD) Single Images	P	Severe DR (SD) Averaged Images	Severe DR (SD) Single Images	P	Proliferative DR (SD) Averaged Images	Proliferative DR (SD) Single Images	P
FAZ size	0.29 (0.10)	0.27 (0.10)	0.507	0.34 (0.14)	0.33 (0.14)	0.888	0.39 (0.17)	0.23 (0.14)	0.034*	0.32 (0.16)	0.28 (0.17)	0.685	0.46 (0.16)	0.27 (0.14)	<0.001*
FAZ circularity	0.76 (0.07)	0.69 (0.08)	0.693	0.60 (0.07)	0.61 (0.05)	0.730	0.54 (0.12)	0.54 (0.11)	0.900	0.41 (0.04)	0.55 (0.08)	0.010*	0.55 (0.15)	0.49 (0.14)	0.244
SRL superior VLD	20.05 (0.92)	21.93 (1.12)	<0.001*	18.50 (0.99)	20.14 (1.14)	0.005*	16.95 (1.21)	18.78 (1.14)	0.003*	17.56 (1.80)	19.42 (1.54)	0.115	16.38 (1.83)	17.79 (1.67)	0.013*
SRL inferior VLD	18.65 (1.65)	21.14 (2.07)	<0.001*	17.87 (0.93)	20.02 (1.06)	<0.001*	17.30 (1.07)	19.03 (1.71)	0.019*	16.39 (1.40)	18.39 (1.22)	0.043*	16.93 (1.78)	18.84 (1.88)	0.002*
SRL nasal VLD	19.59 (0.98)	22.24 (1.13)	<0.001*	18.81 (0.60)	20.60 (1.08)	0.001*	17.84 (1.05)	19.59 (1.66)	0.011*	18.31 (0.69)	20.23 (0.94)	0.006*	16.82 (1.64)	18.21 (1.91)	0.016*
SRL temporal VLD	19.49 (1.36)	21.65 (1.35)	<0.001*	18.15 (0.80)	20.26 (1.17)	<0.001*	17.81 (1.13)	19.15 (1.86)	0.066	17.17 (0.96)	17.89 (1.15)	0.318	16.62 (1.77)	18.11 (1.86)	0.012*
SRL inner ring VLD	19.48 (0.83)	21.75 (1.21)	<0.001*	18.35 (0.55)	20.25 (0.83)	<0.001*	17.45 (0.59)	19.15 (1.20)	0.001*	17.39 (0.91)	18.98 (1.08)	0.036*	16.67 (1.40)	18.22 (1.43)	0.001*
SRL total VLD	18.25 (0.83)	20.66 (1.20)	<0.001*	16.92 (0.69)	19.16 (0.88)	<0.001*	16.11 (0.70)	18.26 (1.15)	<0.001*	16.07 (0.79)	18.11 (0.89)	0.005*	15.40 (1.26)	17.39 (1.30)	<0.001*
DRL superior VLD	21.39 (1.13)	22.39 (1.10)	0.001*	20.08 (1.00)	20.77 (1.23)	0.215	18.00 (1.08)	19.46 (1.05)	0.007*	18.55 (0.98)	19.75 (0.40)	0.036*	17.63 (2.22)	19.33 (1.74)	0.008*
DRL inferior VLD	20.76 (1.28)	22.45 (1.23)	<0.001*	19.15 (0.67)	21.15 (0.60)	<0.001*	18.36 (1.28)	20.05 (0.81)	0.003*	17.01 (1.20)	19.23 (1.79)	0.051	18.14 (1.68)	19.92 (1.63)	0.001*
DRL nasal VLD	20.48 (1.36)	21.75 (1.42)	0.001*	19.38 (1.03)	20.26 (1.24)	0.123	17.63 (1.65)	19.35 (1.40)	0.022*	18.90 (1.24)	20.16 (1.11)	0.130	17.37 (1.83)	18.86 (1.81)	0.012*
DRL temporal VLD	19.80 (1.64)	20.95 (1.37)	0.007*	18.21 (1.36)	19.68 (1.41)	0.038*	17.46 (1.29)	19.28 (1.31)	0.006*	15.36 (0.99)	17.07 (1.32)	0.049*	16.72 (1.85)	18.96 (1.94)	<0.001*
DRL inner ring VLD	20.59 (1.10)	21.88 (1.10)	<0.001*	19.21 (0.79)	20.47 (0.94)	0.007*	17.82 (0.41)	19.53 (0.67)	<0.001*	17.43 (0.58)	19.04 (0.86)	0.008*	17.41 (1.42)	19.25 (1.26)	<0.001*

Variable	Control		No DR		Mild DR		Moderate DR		Severe DR		Proliferative DR		P
	Averaged Images	Single Images	Averaged Images	Single Images	Averaged Images	Single Images	Averaged Images	Single Images	Averaged Images	Single Images	Averaged Images	Single Images	
DRL total VLD	18.55 (1.05)	20.68 (1.01)	18.05 (0.74)	20.32 (0.67)	17.30 (0.78)	19.46 (0.85)	16.31 (0.44)	18.94 (0.68)	15.95 (0.44)	18.45 (0.69)	15.99 (1.09)	18.77 (1.21)	<0.001*
SRL superior PD	0.38 (0.02)	0.41 (0.02)	0.37 (0.01)	0.40 (0.01)	0.36 (0.01)	0.39 (0.02)	0.35 (0.02)	0.38 (0.02)	0.36 (0.03)	0.39 (0.02)	0.34 (0.03)	0.36 (0.03)	0.033*
SRL inferior PD	0.35 (0.03)	0.40 (0.03)	0.35 (0.02)	0.40 (0.02)	0.35 (0.02)	0.39 (0.02)	0.35 (0.01)	0.38 (0.03)	0.33 (0.02)	0.37 (0.01)	0.34 (0.03)	0.38 (0.03)	<0.001*
SRL nasal PD	0.36 (0.02)	0.41 (0.01)	0.37 (0.01)	0.41 (0.02)	0.37 (0.01)	0.40 (0.02)	0.36 (0.02)	0.39 (0.03)	0.37 (0.02)	0.41 (0.01)	0.35 (0.02)	0.37 (0.03)	0.010*
SRL temporal PD	0.37 (0.02)	0.40 (0.02)	0.37 (0.02)	0.41 (0.02)	0.36 (0.01)	0.39 (0.02)	0.37 (0.01)	0.39 (0.03)	0.36 (0.01)	0.37 (0.02)	0.35 (0.03)	0.37 (0.03)	0.044*
SRL inner ring PD	0.36 (0.02)	0.40 (0.02)	0.37 (0.01)	0.40 (0.01)	0.36 (0.01)	0.39 (0.01)	0.36 (0.01)	0.38 (0.02)	0.36 (0.01)	0.39 (0.01)	0.35 (0.01)	0.37 (0.02)	<0.001*
SRL total PD	0.35 (0.01)	0.39 (0.02)	0.34 (0.01)	0.39 (0.01)	0.33 (0.01)	0.37 (0.01)	0.33 (0.01)	0.36 (0.02)	0.33 (0.01)	0.37 (0.01)	0.32 (0.01)	0.35 (0.02)	<0.001*
DRL superior PD	0.39 (0.02)	0.42 (0.02)	0.39 (0.02)	0.42 (0.01)	0.38 (0.02)	0.40 (0.03)	0.37 (0.03)	0.39 (0.03)	0.37 (0.03)	0.39 (0.01)	0.35 (0.04)	0.37 (0.03)	0.040*
DRL inferior PD	0.38 (0.02)	0.42 (0.02)	0.37 (0.02)	0.41 (0.02)	0.37 (0.01)	0.40 (0.01)	0.37 (0.03)	0.39 (0.02)	0.35 (0.03)	0.38 (0.03)	0.36 (0.03)	0.39 (0.03)	0.002*
DRL nasal PD	0.38 (0.02)	0.42 (0.02)	0.38 (0.02)	0.41 (0.02)	0.38 (0.02)	0.40 (0.02)	0.35 (0.04)	0.38 (0.03)	0.39 (0.03)	0.41 (0.03)	0.34 (0.04)	0.36 (0.04)	0.121
DRL temporal PD	0.37 (0.03)	0.40 (0.02)	0.37 (0.02)	0.40 (0.02)	0.36 (0.03)	0.39 (0.03)	0.35 (0.03)	0.38 (0.03)	0.31 (0.02)	0.34 (0.03)	0.33 (0.03)	0.36 (0.04)	0.003*
DRL inner ring PD	0.38 (0.01)	0.42 (0.02)	0.38 (0.01)	0.41 (0.01)	0.37 (0.01)	0.40 (0.02)	0.36 (0.02)	0.38 (0.01)	0.35 (0.01)	0.38 (0.02)	0.34 (0.02)	0.37 (0.02)	<0.001*
DRL total PD	0.34 (0.01)	0.39 (0.01)	0.34 (0.01)	0.39 (0.01)	0.33 (0.01)	0.38 (0.02)	0.33 (0.01)	0.37 (0.01)	0.32 (0.01)	0.37 (0.01)	0.32 (0.01)	0.36 (0.02)	<0.001*

T-test comparing means of quantitative variables for single versus averaged images in control eyes and eyes with varying degrees of diabetic retinopathy (DR) severity. Bold (\*) values denote significance set at P < 0.05.

PD, perfusion density, is defined as the total area covered by perfused vasculature per unit area (%); VLD, vessel length density, is defined as the total length of perfused vasculature per unit area (mm<sup>2</sup>).

DRL = deep retinal layer. FAZ = foveal avascular zone. SD = standard deviation. SRL = superficial retinal layer.

Author Manuscript

Author Manuscript

Author Manuscript

Author Manuscript



**Table 3.**

Association of Averaged and Single Quantitative Metrics with BCVA

Variable	Association with BCVA (Univariate Linear Regression) (Averaged Images)		Association with BCVA (Univariate Linear Regression) (Single Images)	
	Coefficient	P	Coefficient	P
FAZ size	0.211	<b>0.004*</b>	-0.095	0.313
FAZ circularity	-0.223	<b>0.016*</b>	-0.214	<b>0.015*</b>
SRL superior VLD	-0.012	<b>0.004*</b>	-0.015	<b>0.001*</b>
SRL inferior VLD	-0.011	0.055	-0.014	<b>0.008*</b>
SRL nasal VLD	-0.016	<b>0.019*</b>	-0.015	<b>0.003*</b>
SRL temporal VLD	-0.017	<b>0.001*</b>	-0.017	<b>0.002*</b>
SRL inner ring VLD	-0.020	<b>&lt;0.001*</b>	-0.019	<b>&lt;0.001*</b>
SRL total VLD	-0.024	<b>&lt;0.001*</b>	-0.022	<b>&lt;0.001*</b>
DRL superior VLD	-0.017	<b>&lt;0.001*</b>	-0.018	<b>0.001*</b>
DRL inferior VLD	-0.012	<b>0.046*</b>	-0.014	<b>0.038*</b>
DRL nasal VLD	-0.016	<b>0.005*</b>	-0.016	<b>0.012*</b>
DRL temporal VLD	-0.013	<b>0.009*</b>	-0.012	0.058
DRL inner ring VLD	-0.020	<b>&lt;0.001*</b>	-0.021	<b>0.006*</b>
DRL total VLD	-0.025	<b>&lt;0.001*</b>	-0.025	<b>0.004*</b>
SRL superior PD	-0.577	<b>0.046*</b>	-0.943	<b>0.003*</b>
SRL inferior PD	-0.200	0.617	-0.928	<b>0.026*</b>
SRL nasal PD	-0.443	0.366	-0.966	<b>0.020*</b>
SRL temporal PD	-0.798	0.074	-1.032	<b>0.010*</b>
SRL inner ring PD	-1.862	<b>0.007*</b>	-1.624	<b>0.001*</b>
SRL total PD	-2.594	<b>&lt;0.001*</b>	-1.907	<b>&lt;0.001*</b>
DRL superior PD	-0.752	<b>0.004*</b>	-0.941	<b>0.002*</b>
DRL inferior PD	-0.266	0.616	-0.767	0.094
DRL nasal PD	-0.656	<b>0.041*</b>	-0.765	<b>0.018*</b>
DRL temporal PD	-0.653	<b>0.018*</b>	-0.673	<b>0.037*</b>
DRL inner ring PD	-1.488	<b>0.001*</b>	-1.345	<b>0.003*</b>
DRL total PD	-2.190	<b>0.001*</b>	-1.759	<b>0.003*</b>

Results of univariate linear regressions for the ability of listed variables to predict BCVA (logMAR) in patients with DR. (+) coefficient = worse logMAR BCVA versus (-) coefficient = better logMAR BCVA. Bold (\*) values denote significance set at P < 0.05. PD, perfusion density, is defined as the total area covered by perfused vasculature per unit area (%); VLD, vessel length density, is defined as the

total length of perfused vasculature per unit area ( $\text{mm}/\text{mm}^2$ ). BCVA = best corrected visual acuity (in logarithm of the minimum angle of resolution). DRL = deep retinal layer. FAZ = foveal avascular zone.  
SD = standard deviation. SRL = superficial retinal layer.

Author Manuscript

Author Manuscript

Author Manuscript

Author Manuscript

**Table 4.**

Association of Averaged and Single Quantitative Metrics with DR Severity

Variable	Association with DR Severity (Univariate Linear Regression) (Averaged Images)		Association with DR Severity (Univariate Linear Regression) (Single Images)	
	Coefficient	P	Coefficient	P
FAZ size	6.176	<0.001*	0.053	0.980
FAZ circularity	-8.731	<0.001*	-10.107	<0.001*
SRL superior VLD	-0.776	<0.001*	-0.769	<0.001*
SRL inferior VLD	-0.550	<b>0.001*</b>	-0.501	<b>0.003*</b>
SRL nasal VLD	-0.888	<0.001*	-0.711	<0.001*
SRL temporal VLD	-0.759	<0.001*	-0.679	<0.001*
SRL inner ring VLD	-1.043	<0.001*	-0.842	<0.001*
SRL total VLD	-1.072	<0.001*	-0.889	<0.001*
DRL superior VLD	-0.692	<0.001*	-0.809	<0.001*
DRL inferior VLD	-0.746	<0.001*	-0.767	<0.001*
DRL nasal VLD	-0.687	<0.001*	-0.692	<0.001*
DRL temporal VLD	-0.631	<0.001*	-0.580	<0.001*
DRL inner ring VLD	-0.928	<0.001*	-0.972	<0.001*
DRL total VLD	-1.076	<0.001*	-1.025	<0.001*
SRL superior PD	-38.779	<0.001*	-48.615	<0.001*
SRL inferior PD	-8.409	0.471	-22.591	0.076
SRL nasal PD	-27.511	<b>0.012*</b>	-43.087	<0.001*
SRL temporal PD	-26.017	<b>0.016*</b>	-38.738	<0.001*
SRL inner ring PD	-81.947	<0.001*	-63.373	<0.001*
SRL total PD	-89.717	<0.001*	-63.405	<0.001*
DRL superior PD	-32.065	<0.001*	-43.458	<0.001*
DRL inferior PD	-28.909	<b>0.004*</b>	-40.900	<0.001*
DRL nasal PD	-25.168	<0.001*	-33.827	<0.001*
DRL temporal PD	-31.889	<0.001*	-31.376	<0.001*
DRL inner ring PD	-66.395	<0.001*	-61.989	<0.001*
DRL total PD	-92.661	<0.001*	-73.286	<0.001*

Results of univariate linear regressions for the ability of listed variables to predict worse DR severity. (+) coefficient = worse DR severity versus (-) coefficient = less DR severity.

Author Manuscript

Author Manuscript

Author Manuscript

Author Manuscript

DR severity was defined as a categorical variable with 0 = control, 1 = diabetes without retinopathy, 2 = mild non-proliferative DR (NPDR), 3 = moderate NPDR, 4 = severe NPDR and 5 = proliferative DR. Bold (\*) values denote significance set at  $P < 0.05$ . PD, perfusion density, is defined as the total area covered by perfused vasculature per unit area (%); VLD, vessel length density, is defined as the total length of perfused vasculature per unit area ( $\text{mm}/\text{mm}^2$ ). DR = diabetic retinopathy. DRL = deep retinal layer. FAZ = foveal avascular zone. SD = standard deviation. SRL = superficial retinal layer.